

MEASUREMENT OF THE TOTAL CROSS SECTION OF URANIUM-URANIUM COLLISIONS AT $\sqrt{s_{NN}} = 192.8 \text{ GeV}^*$

W. Fischer[†], A.J. Baltz, M. Blaskiewicz, D. Gassner, K.A. Drees, Y. Luo, M. Minty, P. Thieberger, M. Wilinski, Brookhaven National Laboratory, Upton, NY 11973, USA;
I.A. Pshenichnov, Institute for Nuclear Research, Russian Academy of Sciences, Moscow, Russia

Abstract

Heavy ion cross sections totaling several hundred barns have been calculated previously for the Relativistic Heavy Ion Collider (RHIC) and the Large Hadron Collider (LHC). These total cross sections are more than an order of magnitude larger than the geometric ion-ion cross sections, and are primarily due to Bound-Free Pair Production (BFPP) and Electro-Magnetic Dissociation (EMD). Apart from a general interest in verifying the calculations experimentally, an accurate prediction of the losses created in the heavy ion collisions is of practical interest for the LHC, where some collision products are lost in cryogenically cooled magnets and have the potential to quench these magnets. In the 2012 RHIC run uranium ions collided with each other at a center-of-mass energy of 192.8 GeV per nucleon-pair with nearly all beam losses due to collisions. This allows for the measurement of the total cross section and a comparison with calculations.

INTRODUCTION

The total cross sections of colliding heavy ion beams are primarily due to Bound-Free Pair Production (BFPP) and Electro-Magnetic Dissociation (EMD). These have been previously calculated for RHIC [1] and the LHC [2].

Secondary beams from BFPP and EMD can limit the LHC heavy ion luminosity since they have a different charge-to-mass ratio than the primary beam and may be lost in cold magnets. The secondary beams generated in Au–Au and U–U collisions in RHIC are within the transverse momentum aperture but outside the longitudinal acceptance of the radio frequency buckets. These secondary beams are eventually lost, but not in the same turn.

In 2012 RHIC operated for the first time with uranium ions, which have a prolate shape. Collisions of uranium ions along their long axis creates a quark-gluon plasma even denser than that from collisions of the more spherical gold ions. Central collisions of uranium ions with the long axes parallel creates elliptic flow [3] of secondary particles, but without the magnetic field generated by the ions passing each other when the elliptic flow is generated through partial overlap of the ions.

In U–U operation with a low-loss magnetic lattice [4, 5] and 3-dimensional stochastic cooling in store [6], the beam loss of a well-tuned machine is almost entirely due to luminous processes. In this situation the total cross section can be obtained from the observed beam loss rates.

* Work supported by Brookhaven Science Associates, LLC under Contract No. DE-AC02-98CH10886 with the U.S. Department of Energy.

[†] Wolfram.Fischer@bnl.gov

CALCULATED TOTAL CROSS SECTION

The calculated U–U cross sections at RHIC are shown in Table 1 together with the RHIC Au–Au and LHC Pb–Pb cross sections. The largest contributions to these cross sections come not from the nuclear overlap of the colliding ions, but from two electromagnetic processes, bound electron free-positron pair (BFPP) production and electromagnetic dissociation (EMD) of the nucleus. Bound electron-positron-pair production changes the charge of the ion causing it to fall out of the beam. Electromagnetic dissociation removes at least one neutron from the ion, changing its mass and likewise causing it to fall out of the beam.

Since the total U–U cross section measured here is obtained from beam loss rates, processes that do not lead to beam loss are not included in the calculation. At RHIC energies the infinite elastic Coulomb scattering cross section does not cause any notable deviation in the beam trajectories. The U–U cross section for free electron positron pairs in this experiment is huge, 64 kb calculated in the perturbative formula of Racah [7] (a formula which agrees very well with recent numerical calculation and is much more accurate than the formula of Landau and Lifshitz [8]). For Au–Au at RHIC the corresponding perturbative cross section is 36 kb. However, these free pair cross sections are almost completely dominated by soft pairs, where the ions remain intact, and they do not contribute to the present measured total cross section.

Table 1: Calculated Total Cross Sections for Au–Au and U–U Collisions in RHIC, and Pb–Pb Collisions in the LHC

collider species		RHIC Au–Au	RHIC U–U	LHC Pb–Pb
$\sqrt{s_{NN}}$	GeV	200	192.8	5520
BFPP	b	117	329	272
single EMD	b	94.15	150.1	215
nuclear	b	7.31	8.2	7.9
total	b	218.46	487.3	503.9

RHIC IN U–U OPERATION

In 2012 uranium ions were collided for the first time because the new Electron Beam Ion Source [9] was recently commissioned. The magnetic lattice was selected to provide a large dynamic aperture for on- and off-momentum particles with a slightly raised β^* [4]. Table 2 shows the main beam parameters. A total of 60 stores were provided, with an average store length of 6.4 h.

2012 was also the first year with full 3-dimensional stochastic cooling in both rings. The cooling was so strong (Fig. 1) that emittances were reduced by a factor of four, the

Table 2: Main Beam Parameters During U–U Operation. Values given are typical for the highest luminosity stores.

parameter	unit	value	
		initial	at \mathcal{L}_{max}
beam energy E	GeV/nucleon	96.4	
number of bunches n	...	111	
bunches colliding at IP6 n_{c6}	...	102	
bunches colliding at IP8 n_{c8}	...	111	
bunch intensity N_b	10^9	0.3	0.27
beam current I_b	mA	38	34
rms emittance ε_{xy}	μm	2.25	0.40
luminosity \mathcal{L}/IP	$10^{26} \text{ cm}^{-2}\text{s}^{-1}$	3	9
absolute beam loss rate \dot{N}	1000/s	350	900
relative beam loss rate \dot{N}/N	%/h	4	10

peak luminosity increased by a factor of three, and the average store luminosity increased by a factor of five. The low-loss lattice and the cooling resulted in beam losses (also visible in Fig. 1) nearly exclusively from burn-off.

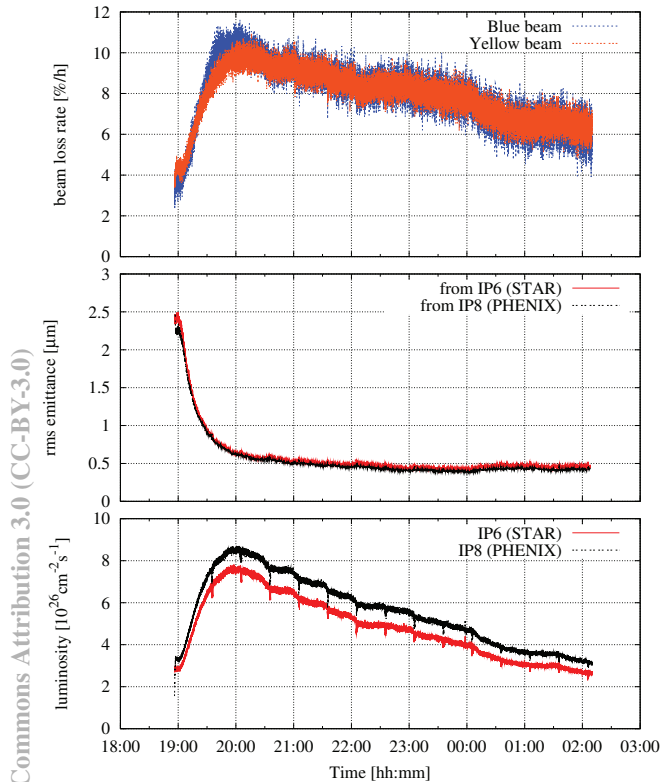


Figure 1: U–U store (fill 16858) with beam loss rates (top), rms emittances (middle), and luminosities (bottom). The reduction in the emittances and the corresponding increase in the luminosity is due to stochastic cooling.

CROSS SECTION MEASUREMENT

In the case where all beam losses are given by the total U–U cross section σ_{tot} we have

$$\frac{dN_B(t)}{dt} = \frac{dN_Y(t)}{dt} = -[\mathcal{L}_6(t) + \mathcal{L}_8(t)] \sigma_{tot} \quad (1)$$

where $N_{B,Y}$ are the Blue and Yellow beam total intensities, and $\mathcal{L}_{6,8}(t)$ the instantaneous luminosities at IP6 (STAR) and IP8 (PHENIX) respectively. The total cross section is

then given by

$$\sigma_{tot} = -\frac{\dot{N}_{B,Y}(t)}{[\mathcal{L}_6(t) + \mathcal{L}_8(t)]} \quad (2)$$

and, neglecting timing errors, the systematic error by

$$\Delta\sigma^{sys} = \sigma_{tot} \left(\frac{\Delta N_{B,Y}^{sys}}{N_{B,Y}} + \frac{\Delta\mathcal{L}_6^{sys} + \Delta\mathcal{L}_8^{sys}}{\mathcal{L}_6 + \mathcal{L}_8} \right). \quad (3)$$

We need to obtain the beam loss rates $\dot{N}_{B,Y}$ and the luminosities $\mathcal{L}_{6,8}$ for the determination of the total cross section σ_{tot} via Eq. (2). The beam loss rate is calculated from a time-dependent measurement of the total beam intensity with a DCCT. The luminosity is measured via the detection of neutron pairs in time-coincidence in the Zero Degree Calorimeter (ZDC) [10].

Luminous and Non-luminous Losses

A principal limitation of the method used here comes from the fact that there can be beam losses from other processes than U–U interactions given by the total cross section σ_{tot} . In a situation with non-luminous losses, the use of equation (2) will only give an upper limit for σ_{tot} . There are a number of processes that can lead to non-luminous beam losses, namely intrabeam scattering, residual gas elastic scattering, dynamic aperture and beam-beam effects, and residual gas inelastic scattering. Emittance growth processes with time scales of 1 h or longer are counteracted by stochastic cooling and will not lead to particle loss. But we must expect that there are a small number of particles lost through other processes than burn-off, and our analysis needs to take this into account.

The predominant non-luminous loss process is inelastic scattering on the residual gas, leading to beam loss rates of which are about 10% of the total loss rate at the beginning of the store, and 3% at the time of \mathcal{L}_{max} (Table 3, Fig. 2).

Table 3: U Beam Loss Rate from Residual Gas Scattering with with Parameters Given in Table 2

parameter	unit	value
<i>warm vacuum sections</i>		
length per ring l_w	m	652
gas temperature	K	300
average pressure $\langle P \rangle$	nTorr	0.5
static gas composition	...	95% H ₂ , 5% CO
N ₂ equivalent pressure	nTorr	0.5
emittance growth time τ_{ε_n} , at \mathcal{L}_{max}	h	49
<i>beam loss from residual gas inelastic scattering</i>		
coefficient for beam loss on N ₂	s ⁻¹ Torr ⁻¹	800
N ₂ equivalent pressure	nTorr	0.1
beam lifetime $\tau_N = N_{B,Y}/\dot{N}_{B,Y}$	h	498
loss rate $\dot{N}_{B,Y}$, initial	1000 s ⁻¹	19

Measurement Value and Statistical Error

There were 60 physics U–U stores with an average length of 6.4 h. As a first step we selected all stores which did not have any unusually high beam losses, and in which \dot{N}_B and \dot{N}_Y were approximately equal and proportional to the total luminosity $\mathcal{L}_6 + \mathcal{L}_8$ for at least a period of the store. These were the last 50 of all 60 physics stores.

For each of these stores a fitted value for σ_{tot} was obtained by assuming that all losses are luminous, i.e. by fitting a straight line to (\dot{N}, \mathcal{L}) with a zero offset (Fig. 2).

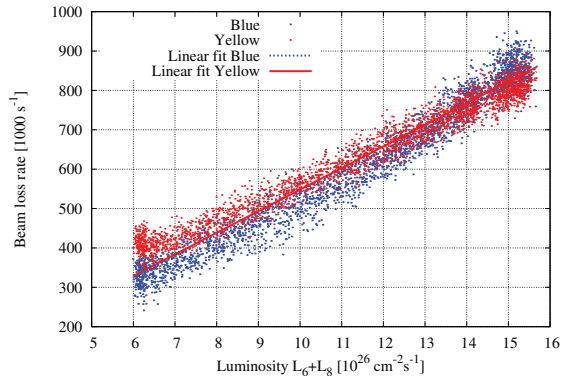


Figure 2: Beam loss rates as a function of the total luminosity $\mathcal{L}_6 + \mathcal{L}_8$ (fill 16858). Fitted values for this case are $\sigma_{tot} = (506.90 \pm 0.21)$ barn for Blue, and $\sigma_{tot} = (539.37 \pm 0.16)$ barn for Yellow. The error is the statistical standard error.

An analysis of the so fitted σ_{tot} revealed that the earlier stores show a much larger fitted σ_{tot} value than the later stores, indicating that not all beam losses were luminous. We note that transverse stochastic cooling became available only in later stores and we further restricted our data selection to these stores. But even for those fills we cannot be sure that all losses are luminous.

In a second step we fitted σ_{tot} to the (\dot{N}, \mathcal{L}) data points for all later stores under the assumption that there are residual beam losses, i.e. with a nonzero offset. In Fig. 3 we show the fitted values for both σ_{tot} and the residual beam loss rates, where we restricted the data selection to data points with a residual beam loss rates not larger than 30000 s^{-1} , about 10% of the minimum and 3% of the maximum beam loss rates observed (see Fig. 2), as to ensure that the σ_{tot} determination is done with conditions of nearly all beam losses due to burn-off.

Combining the individual data points in Fig. 3 yields the measurement value and statistical error as $\sigma_{tot} = (505 \pm 13^{stat})$ barn. We have calculated the statistical error simply as the standard deviation of the σ_{tot} distribution since this distribution is much wider than the statistical errors for the individual data points.

Measurement Systematic Error

If timing errors can be neglected, the systematic error σ^{sys} is given by Eq. (3), and is determined by the systematic errors of the beam intensity and luminosities. The estimated errors of all components are summarized in Table 4, and the total is obtained as the quadratic addition as $\sigma^{sys} = 39$ barn (see also [11]). We are still investigating methods to reduce the systematic errors.

SUMMARY

In U-U stores with 3D stochastic cooling nearly all beam losses are from burn-off and the total interaction cross sec-

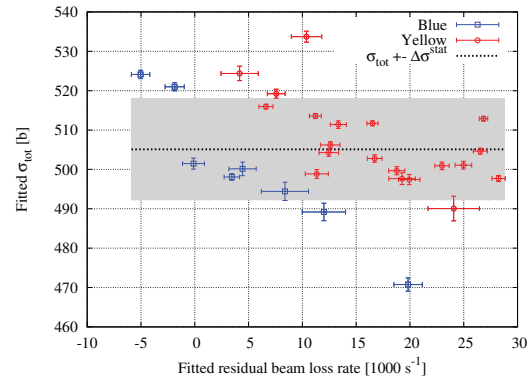


Figure 3: Fitted σ_{tot} and residual beam loss rates for selected stores. The errors of the individual data points are the standard errors from the linear fit.

Table 4: Sources and Contributions to $\Delta N_{B,Y}^{sys}/N_{B,Y}$ (left) and $\Delta \mathcal{L}^{sys}/\mathcal{L}$ (right)

source	error	source	error
temp. variations	0.19%	beam displacement	4.0%
bunch pattern	0.10%	crossing angle	2.0%
calibration error	0.15%	intensity	6.0%
PCT accuracy, drifts	0.30%	beam-beam	0.5%
output noise	0.01%	hysteresis	1.0%
		bunch pattern	2.0%
total $\Delta N_{B,Y}^{sys}/N_{B,Y}$	0.40%	total $\Delta \mathcal{L}^{sys}/\mathcal{L}$	7.8%

tion can be obtained from the observed beam loss rates as

$$\sigma_{tot}^{meas} = (505 \pm 13^{stat} \pm 39^{sys}) \text{ barn.} \quad (4)$$

This result agrees, within the estimated errors, with the calculated total cross section $\sigma_{tot}^{calc} = 487.3$ barn. The effort to reduce the systematic error estimate of the measurement is still ongoing.

ACKNOWLEDGMENTS

The authors are thankful for discussions and support to J. Bergoz, S. Binello, R. Bruce, W. Christie, T. Hayes, X. He, M. Mapes, K. Smith, and J. Jowett.

REFERENCES

- [1] H. Gould, LBL-18593 (1984); A.J. Baltz, M.-J. Rhoades-Brown, and J. Wesener, Phys. Rev. E **54**, 4233 (1996).
- [2] S.R. Klein, NIM A **459**, 51 (2001); J.M. Jowett, J.-B. Jeanneret, and K. Schindl, PAC 2003 pp. 1682-1684 (2003).
- [3] K.H. Ackermann et al. (STAR collaboration), Phys. Rev. Lett. **86** (2001), pp. 402.
- [4] Y. Luo et al., IPAC 2012, pp. 175-177 (2012).
- [5] Y. Luo et al., these proceedings, TUPFI082.
- [6] M. Blaskiewicz and J.M. Brennan, PRSTAB **10**, 061001 (2007); M. Blaskiewicz, J.M. Brennan, and F. Severino, PRL **100**, 174802 (2008); M. Blaskiewicz, J.M. Brennan, and K. Mernick, PRL **105**, 094801 (2010).
- [7] G. Racah, Nuovo Cimento **14**, 93 (1937).
- [8] L.D. Landau, E.M. Lifshitz, Phys. Z. Sowjetunion **6**, 244 (1934).
- [9] J.G. Alessi et al., PAC 2011, pp. 1966-1968 (2011).
- [10] C. Adler et al., NIM A **470**, pp. 488-499 (2001).
- [11] Simon White, CERN-THESIS-2010-139, p. 87 (2010).